

# UC Berkeley

## UC Berkeley Previously Published Works

### Title

HIGH-TEMPERATURE BATTERIES.

### Permalink

<https://escholarship.org/uc/item/8755p7jn>

### Authors

Cairns, EJ  
Dunning, JS

### Publication Date

1976

Peer reviewed



RESEARCH PUBLICATION • GMR-2065

## HIGH-TEMPERATURE BATTERIES

Elton J. Cairns  
John S. Dunning

Electrochemistry Department

January 23, 1976



HIGH-TEMPERATURE BATTERIES

by

Elton J. Cairns and John S. Dunning  
Electrochemistry Department  
Research Laboratories, General Motors Corporation  
Warren, Michigan 48090

January 23, 1976

For presentation to the High-Temperature Battery Workshop,  
Argonne National Laboratory, Argonne, Illinois, March 23, 1976,  
and for publication in the Proceedings of the Workshop.

# HIGH-TEMPERATURE BATTERIES

by

Elton J. Cairns and John S. Dunning  
Research Laboratories, General Motors Corporation  
Warren, Michigan 48090

## ABSTRACT

The state of the art for high-temperature batteries will be presented and discussed. Emphasis will be given to the lithium alloy/metal sulfide and sodium/sulfur cells. Other systems to be considered include lithium/chlorine and sodium/metal halide. Cell chemistry and performance and life-limiting factors will be reviewed for all of the systems, and the status of investigations in critical problem areas will be given. Recent advances in the demonstration of high specific energy and expectations for future improvement will be presented.

## INTRODUCTION

The current awareness of the developing shortage of inexpensive sources of energy has given new impetus to the search for and development of means for making more effective and more efficient use of the energy sources and energy conversion systems that we possess. The most rapidly-growing sector of our energy economy is that of electrical energy generation. Fortunately, we possess the capability of generating electrical energy from a wide variety of primary fuels, including coal and nuclear fuel, which are in much larger supply in the United States than petroleum. In order to more effectively utilize our electrical energy system, it is important to have an efficient, flexible, economical means of storing off-peak electrical energy for later use during peak demand periods. In addition, the demand for petroleum could be reduced by the use of rechargeable batteries as a power source for automobiles.

The performance, lifetime, and cost goals for the battery applications mentioned above tend to exclude all of the presently-available batteries, and many proposed batteries. The class of batteries which is projected to have the best combination of performance, life, and cost for large-volume application in multikilowatt sizes is that of high-temperature batteries, which are being developed to meet the following general goals:

	Peak Specific Power (W/kg)	Specific Energy* (W·h/kg)	Minimum Cycle Life	Minimum Lifetime (yr)	Cost (\$/kW·h)
Off-peak energy storage	15-50 <sup>†</sup>	100-200 <sup>†</sup>	1000-2000	5	20
Automobiles	200	200	500-1000	3	20

<sup>†</sup> not very important for this application

\* at 50 W/kg

Of course, only those systems using abundant materials can be considered for widespread use.

In the field of high-temperature cells, there are two types of electrolytes in use: molten salts (almost exclusively alkali halides), and solids (almost exclusively sodium-ion conductors). Nearly all of the cells with molten-salt electrolytes use lithium as the reactant at the negative electrode (usually as an alloy) because other candidate reactants are relatively soluble in their molten salts. All of the cells with solid electrolytes use sodium as the negative electrode reactant because the only solid electrolytes of adequate conductance for a low electronegativity metal conduct only sodium ions. The positive electrode reactants are elements of high electronegativity and low equivalent weight, or compounds containing them. These conditions result in the focusing of effort on the following systems: lithium/alkali halide/metal sulfide (or sulfur), sodium/solid electrolyte/sulfur, sodium/solid electrolyte/metal halide, lithium-aluminum/alkali halide/carbon- $\text{TeCl}_4$ , and lithium/alkali halide/chlorine.

In the sections that follow, the systems just listed will be discussed, with emphasis on current status (based on the latest publicly available information) and problems remaining to be solved.

#### LITHIUM/METAL SULFIDE CELLS

The current efforts on lithium/metal sulfide cells evolved from earlier work on lithium/sulfur cells,<sup>1-3</sup> which experienced gradual loss of sulfur from the positive electrode and a corresponding decline in capacity. The use of a sulfur compound such as  $\text{FeS}_2$ ,  $\text{FeS}$ , or  $\text{Cu}_2\text{S}$  reduces the solubility of sulfur-bearing species in the electrolyte, and provides for greatly improved stability of operation without capacity loss,<sup>4-6</sup> at the expense of cell voltage (tenths of a volt) and lower specific energy. (Compare the values in Table I to 2600 W·h/kg for Li/S.)

Table I. PERFORMANCE SUMMARY - HIGH TEMPERATURE BATTERIES

System	Theoretical Specific Energy W·h/kg	Operating Temperature °C	Small Cell Tests (<20 A·h)					Large Cell or Battery Tests (>20 A·h)			
			Capacity Density A·h/cm <sup>2</sup>	Density g A/cm <sup>2</sup>	Peak Power Density W/cm <sup>2</sup>	Cycle Life	Lifetime h	Specific Energy W·h/kg*	Specific Power W/kg	Cycle Life	Lifetime h
Li/LiCl-KCl/FeS <sub>2</sub>	1321	400-450	0.4	0.4	1.4	92	800	-	-	115	617
Li/LiCl-KCl/FeS	869	400-450	-	-	-	-	-	-	-	-	-
Li-Al/LiCl-KCl/FeS <sub>2</sub>	650	400-450	0.65	0.64	(1.0)	300	6400	80-150	8-80	300	6400
Li-Al/LiCl-KCl/FeS	458	400-450	0.75	0.64	0.8	(300)	(5000)	70-85	8-150	121	3700
Li <sub>4</sub> Si/LiCl-KCl/FeS <sub>2</sub>	944	400-450	-	-	-	-	-	-	-	-	-
Li <sub>4</sub> Si/LiCl-KCl/FeS	637	400-450	-	-	-	-	-	-	-	-	-
Na/B-Al <sub>2</sub> O <sub>3</sub> /S*	758	300-400	1.7	0.16	0.3	-	-	77	154	N.A.	N.A.
Na/B-Al <sub>2</sub> O <sub>3</sub> /S**	521	300-400	-	-	-	-	-	-	-	-	-
Na/B-Al <sub>2</sub> O <sub>3</sub> /Na <sub>2</sub> S <sub>1.2</sub> ***	308	300-400	-	-	-	8500	10000 (1000 A·h/cm <sup>2</sup> )	-	-	-	-
Na/B-Al <sub>2</sub> O <sub>3</sub> /NaAlCl <sub>4</sub> -M <sub>x</sub> Cl <sub>y</sub>	792-1034	210	0.4	0.015	0.375	>200	5000 (>60 A·h/cm <sup>2</sup> )	-	-	-	-
Li-Al/LiCl-KCl/C-TeCl <sub>4</sub>	N.A.	400	-	-	-	200	-	60-80	468	100	288
Li/LiCl-KCl-LiF/Cl <sub>2</sub>	2167	450	0.33	1.05	>2.8	325	650	277 <sup>++</sup>	230 <sup>++</sup>	210	668

\* Reaction to Na<sub>2</sub>S<sub>3</sub>

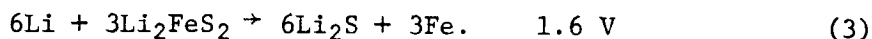
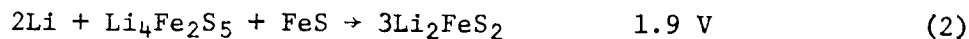
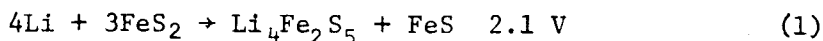
Excluding weight of thermal insulation

\*\* Reaction to Na<sub>2</sub>S<sub>5.2</sub>

Excluding weight of case, insulation, and Cl<sub>2</sub> storage

\*\*\* Reaction in the single phase region  
Na<sub>2</sub>S<sub>5.2</sub> + Na<sub>2</sub>S<sub>3</sub>

Introduction of a metal sulfide in place of sulfur modifies the chemistry of the cell reactions. For the Li/LiCl-KCl/FeS<sub>2</sub> cell, the predominant discharge reactions and corresponding potentials (vs. Li) are:



The theoretical specific energy for these cell reactions is 1321 W·h/kg, about half that for the Li/S cell, largely because of the weight of the Fe.

Each of the above reactions is associated with a plateau in the voltage-capacity curve for the cell, as shown in Fig. 1. Reaction 1 is associated with the upper plateau, Reaction 2 with the small second plateau, and Reaction 3 with the longer plateau near 1.6 V. All of the compounds in Reactions 1-3 have been identified in the electrodes of cells that had been cycled and then examined at the appropriate state of charge.<sup>7,8</sup> It is difficult to return to the fully charged state in which only FeS<sub>2</sub> is present, but little loss of capacity is evident. Even though the reactions above appear to be rather complex, FeS<sub>2</sub> electrodes have demonstrated stable operation for extended time periods.<sup>9</sup>

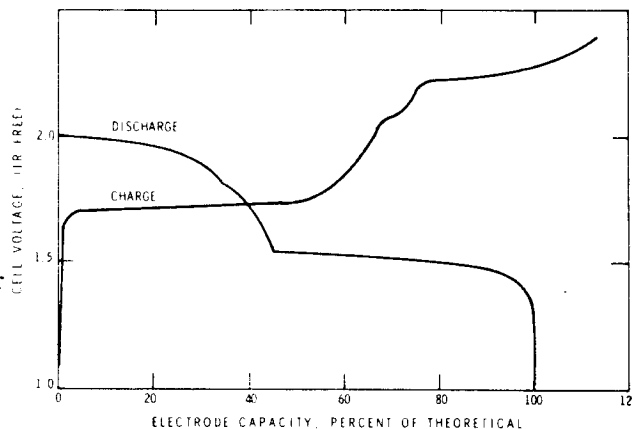
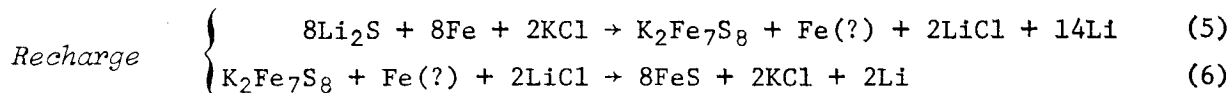
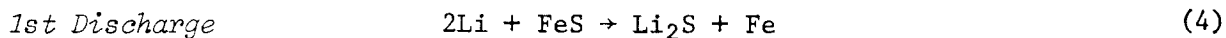


Fig. 1. Voltage-capacity curve for a Li/FeS<sub>2</sub> cell.

Another cell under investigation makes use of FeS in the positive electrode. The most commonly used electrolyte with FeS is the LiCl-KCl eutectic. For the Li/LiCl-KCl/FeS cell, the reactions appear to be:



The leftover iron in Reaction 5 has not been found conclusively, but has been included in the reactions to preserve the 1:1 ratio of iron and sulfur. The compound K<sub>2</sub>Fe<sub>7</sub>S<sub>8</sub>\* has been identified in large amount in electrodes from cycled cells.<sup>8,9</sup> Reaction 6 only proceeds with some difficulty, and K<sub>2</sub>Fe<sub>7</sub>S<sub>8</sub> probably is the major reactant at the positive electrode of the Li/LiCl-KCl/FeS cell after the initial discharge. The voltage-capacity curve for this cell is characterized by a single, flat plateau at 1.5-1.6 V. It is interesting that K<sub>2</sub>Fe<sub>7</sub>S<sub>8</sub> is not an important phase in the FeS<sub>2</sub> electrode, and that Li<sub>2</sub>FeS<sub>2</sub> is not important in the FeS electrode (with LiCl-KCl

\* The exact formula for this compound is in doubt, but this is the best available.

electrolyte). The theoretical specific energy of the Li/FeS cell is 869 W·h/kg. Improvements in stability of operation can also be obtained with other metal sulfides, such as  $\text{Cu}_2\text{S}$ ,<sup>6</sup>  $\text{NiS}$ ,<sup>8</sup>  $\text{CoS}$ ,<sup>8</sup> and  $\text{CuFeS}_2$ ,<sup>8</sup> but the theoretical specific energies for these Li/MS cells are lower than for Li/FeS<sub>2</sub> cells, and these materials are more expensive than FeS<sub>2</sub> or FeS.

Liquid lithium electrodes have not been as stable as desired, because of capacity loss related to both physical and chemical losses of lithium from the electrode.<sup>10</sup> The physical losses are caused by a lack of sufficient wetting of the current collector during recharge, and inadequate wicking of the deposited lithium into the current collector. Various additives to the lithium have been evaluated in an attempt to improve the wetting and wicking properties of the lithium electrode. Chemical losses of lithium from open cells with LiCl-KCl electrolyte have been experienced because of the displacement reaction



and the evaporation of potassium. The rates of both of the above losses have been reduced significantly by the proper choices of current collector materials (nickel, stainless steel, low carbon steel), additives (e.g., copper, zinc), and the use of sealed cells or potassium-free electrolytes (to avoid the potassium-loss mechanism). Even so, further work is necessary before liquid lithium electrodes are acceptable for stable, long-lived cells.

As an alternative to the liquid lithium electrode, the solid lithium-aluminum alloy electrode has been investigated, and shows good stability, at the cost of a lower cell voltage (by about 0.3 V over a large composition range, ~7 a/o to 45 a/o Li) and a greater weight (about 80 w/o of the fully charged electrode is aluminum).<sup>11,12</sup> Compare the theoretical specific energies of corresponding cells in Table I with lithium and lithium-aluminum electrodes, which show a loss of 50%. In addition, some of the lithium in the lithium-aluminum alloy is not available at reasonable current densities (20-30% unavailable at 0.1 A/cm<sup>2</sup>) in contrast to the liquid lithium electrode which exhibits essentially 100% utilization. The best operation of these electrodes is found at an electrolyte volume fraction of 0.2 in the electrode.

Solid lithium-silicon is also under investigation as a negative electrode,<sup>13</sup> and at a composition of  $\text{Li}_4\text{Si}$ , shows a significant weight advantage over  $\text{LiAl}$ , as indicated by the theoretical specific energy values in Table I. Since silicon is not as good an electronic conductor as aluminum, a more elaborate current collector probably will be required for  $\text{Li}_4\text{Si}$ . Voltage plateaus were found at 48, 158, 280, and 336 mV vs. Li at 400°C, in locations consistent with the existence of compounds of the following stoichiometries:  $\text{Li}_5\text{Si}$ ,  $\text{Li}_{4.1}\text{Si}$ ,  $\text{Li}_{2.8}\text{Si}$ , and  $\text{Li}_2\text{Si}$ . No information was presented concerning the ability of the electrode to support current. Lithium-boron alloys have also been investigated,<sup>9,14</sup> and are able to support high discharge current densities (up to 8 A/cm<sup>2</sup>) at 500°C in LiCl-KCl. Performance is much poorer at lower temperatures. Little information is available on recharge characteristics or cycle life,<sup>9</sup> but it appears that it is difficult to remove lithium from the composition  $\text{LiB}_2$ .

The scaleup and engineering efforts on lithium-aluminum/iron sulfide cells have progressed to the point of performance and cycle-life measurements on lightweight cells of about 100 A·h capacity,<sup>8,9,11</sup> of the design shown in

Fig. 2. These cells have typically been operated at current densities in the range 0.04 to 0.25 A/cm<sup>2</sup>, corresponding to complete discharge in 4 to 24 h, which is in the range of interest for off-peak energy storage. The cell weights have been near 1 kg, corresponding to a specific energy of 100 to 150 W·h/kg (see Table I and Fig. 2). Repeated cycling of these cells has shown the capacity retention to be good. Lifetimes of more than 3000 h have been demonstrated for these lightweight Li-Al/LiCl-KCl/FeS<sub>2</sub> cells.<sup>9</sup> In tests involving heavier cells with larger amounts of electrolyte, lifetimes as long as 6400 h have been achieved.<sup>12</sup> Prismatic cells, of vertical orientation with similar capacities (~100 A·h) are also being developed.

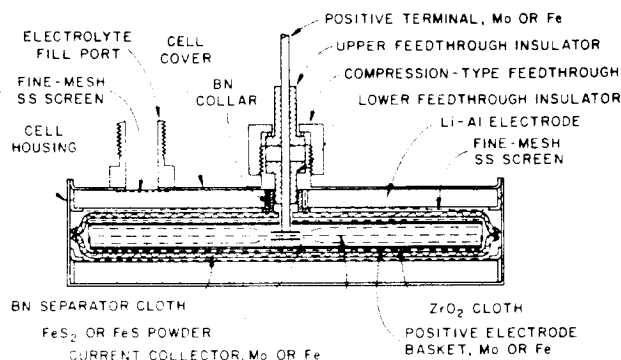


Fig. 2. Lightweight Li-Al/MS cell design. Cell diameter ~13 cm, weight 1-1.7 kg.<sup>9</sup>

The factors which are serving to limit the performance of Li-Al/FeS and Li-Al/FeS<sub>2</sub> cells include swelling of the positive electrode (especially of the FeS cells) which accompanies discharge of the cell. The swelling of the FeS electrode has been associated with the formation of K<sub>2</sub>Fe<sub>7</sub>S<sub>8</sub>. Prevention of the formation of this phase by elimination of potassium from the electrolyte should reduce the amount of swelling.

Incomplete utilization of the FeS or FeS<sub>2</sub> has been a problem, and is at least partially caused by inadequate current collection within the positive electrode. The use of CoS<sub>2</sub> (or CoS) improves the electronic conductivity of the active material,<sup>15</sup> reducing the current collector requirement so that 40-60% utilization can be obtained at 0.1 A/cm<sup>2</sup>, and 415°C. It has also been found that CuS added to FeS (in amounts near 40 w/o) improves the utilization of the active material,<sup>9</sup> and probably reduces the extent of formation of K<sub>2</sub>Fe<sub>7</sub>S<sub>8</sub>, (and perhaps the extent of swelling as well). Further improvement in utilization of the active material is necessary especially at the higher current densities required for automobile propulsion. Values near 70% utilization at 0.4 A/cm<sup>2</sup> and 450°C are desired for this application.

Inexpensive, corrosion-resistant current collectors for FeS and FeS<sub>2</sub> electrodes are needed. Various forms of carbon have been used with some success, but carbon has only a marginally-acceptable electronic conductivity, poor strength, and is not easy to join to other materials. Tungsten and molybdenum have also been used, but they are heavy and expensive. A large number of candidate materials have been evaluated for possible use in Li/S and Li/MS cells, with only a few showing reasonable corrosion resistance, as indicated in Table II.<sup>8,16</sup>

The development of a lightweight, corrosion-resistant feedthrough for sealed cell operation requires an electronic insulator which will remain stable at potentials near that of lithium. Many ceramics have been rejected because they are readily attacked by lithium. The most promising materials currently being investigated are high-purity boron nitride and high-purity aluminum nitride. High-purity BeO is also good but poses a health question. Yttria and some double metal oxides may prove to be acceptable (e.g., CaZrO<sub>3</sub>,



Table II. COMPATIBILITY OF PROSPECTIVE POSITIVE ELECTRODE MATERIALS  
IN LITHIUM/IRON SULFIDE CELLS

Material	Positive Electrode	Results of Corrosion Tests or Cell Tests
Mo	FeS <sub>2</sub> , FeS	Little or no attack of properly prepared material
W	FeS <sub>2</sub>	
C, Graphite	FeS <sub>2</sub> , FeS	
TiN } Coating on Fe	FeS <sub>2</sub>	
FeB }		
Fe	FeS	Moderate attack or dissolution
Ni	FeS	
Fe	FeS <sub>2</sub>	Severe attack or dissolution
Ni	FeS <sub>2</sub>	
Cu	FeS	
Nichrome	FeS <sub>2</sub>	
Nb	FeS <sub>2</sub>	

MgAl<sub>2</sub>O<sub>4</sub>), but more work remains in this area. Bonding techniques are required for the most compact feedthroughs. The conductor of the feedthrough which operates at positive electrode potential must resist oxidation at these high potentials, and must be joined with low resistance to the electrode. The most popular materials for this use are molybdenum and tungsten. Molybdenum is attacked slowly, and both metals are heavy. At present, mechanical feedthroughs are commonly used, but they leave something to be desired in terms of size, weight, and leak rate.

Next in importance to the improvements in the positive electrodes indicated above are better separators. Boron nitride cloth, about 2 mm thick, together with zirconia cloth 1 mm thick has been used most successfully as a separator, preventing contact between the positive and negative electrodes, and helping to retain particles of active material. Thinner, less expensive, and highly corrosion resistant materials are needed for this purpose. Thinner, nonwoven, high purity boron nitride may serve well, if developed. The separator should have very small pores (a few micrometers or less) in order to prevent movement of fine particles of lithium-aluminum, iron, and other solids from the electrodes. It must be thinner (perhaps 1 mm thick) in order to reduce the internal resistance of the cell, and should not be sensitive to air or moisture (for ease in handling and cell assembly). Yttria may be another good candidate. It has shown good stability in preliminary tests, is thermodynamically stable, but is not yet available as a strong, flexible, high-purity cloth or mat.

As a convenience in cell assembly (and as a cost-saving measure), it would be advantageous to develop a simple means for assembling cells in the discharged state (using Fe and Li<sub>2</sub>S in the positive electrode) avoiding the need for metallic lithium and the handling of it. Some experiments have been performed on the assembly and startup of discharged cells, with promising results.

The outlook for the continued development of cells with lithium alloy negative electrodes and iron sulfide positive electrodes is good. It is likely that within the next few years, cells can be developed having specific energies approaching 200 W·h/kg at a specific power of 100 W/kg with a life of over 5000 h and 1000 cycles using FeS<sub>2</sub> electrodes, and 140 W·h/kg at a specific power of 60 W/kg and a life of over 5000 h and 1000 cycles using FeS electrodes. The cost will probably continue to be high (compared to \$20/kW h) until inexpensive feedthroughs, current collectors, and separators are available. Figure 3 shows a conceptual design for a 43 kW·h, 270 kg Li-Al/FeS<sub>2</sub> battery for electric vehicle propulsion.

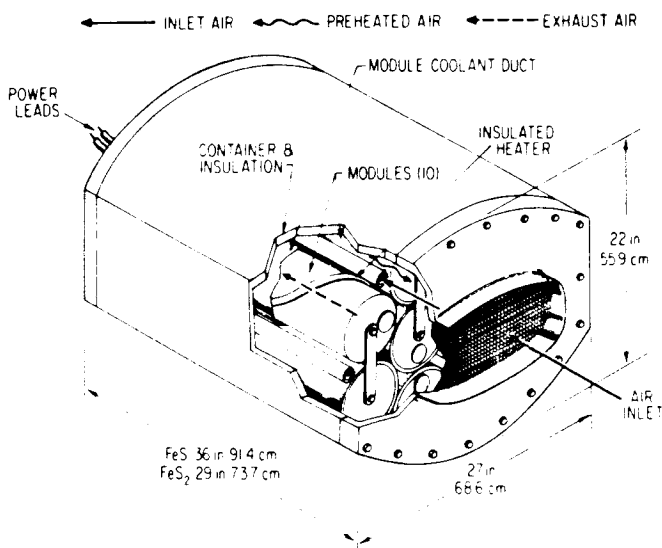


Fig. 3. Conceptual design of an electric vehicle battery using Li-Al/MS cells.<sup>17</sup>

#### SODIUM/SULFUR CELLS

In 1967, the Ford Motor Company<sup>18</sup> revealed their work on the development of a sodium/sulfur cell with a ceramic, sodium-ion-conducting electrolyte. This cell is appealing because it is very simple in concept: molten sodium separated from molten sulfur by a ceramic electrolyte, penetrable only by sodium ions, as shown in Fig. 4.<sup>19</sup> The cell operates at 300-400°C, sodium serves as its own current collector and a carbon felt serves as the current collector for the sulfur electrode.

The overall electrode and cell reactions are rather simple:

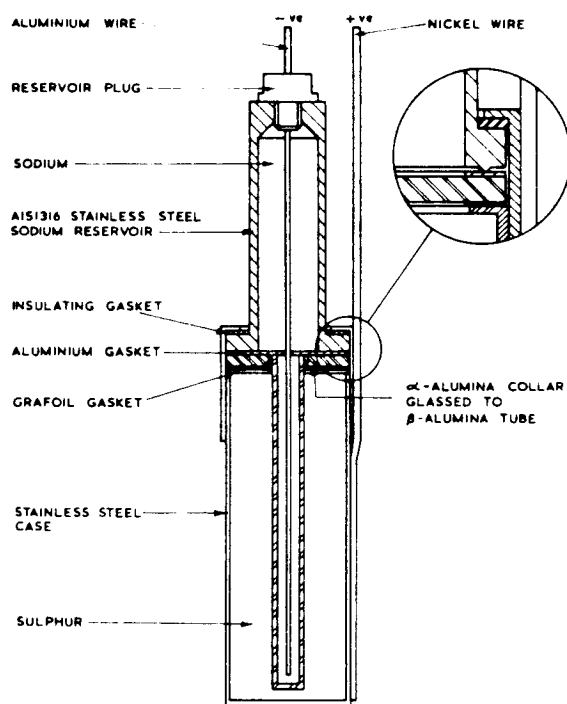
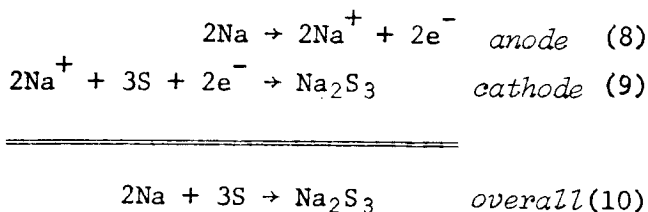


Fig. 4. Conceptual design of a tubular Na/S cell.<sup>19</sup>

The  $\text{Na}_2\text{S}_3$  is not a compound, but merely the stoichiometry at which the compound  $\text{Na}_2\text{S}_2$  begins to precipitate from the sodium polysulfide melt at operating temperature. The phase diagram of the Na-S system shows that at  $350^\circ\text{C}$ , as the sulfur electrode receives sodium during the discharge reaction, a separate liquid phase,  $\text{Na}_2\text{S}_{5.2}$  forms, causing a voltage plateau at 2.07-2.08 V vs. Na, extending from essentially pure sulfur to  $\text{Na}_2\text{S}_{5.2}$ . As more Na is added to  $\text{Na}_2\text{S}_{5.2}$ , the voltage declines through a single-phase region, until the composition  $\text{Na}_2\text{S}_3$  is reached, at which point  $\text{Na}_2\text{S}_2$  begins to precipitate. This is the end of discharge.

The details of the sulfur electrode reactions are rather complex because two sulfur-containing phases and many sulfur-containing species are involved in both chemical and electrochemical reactions. The present state of knowledge of the reactions is as follows.<sup>20</sup> The major species in the polysulfide melt are believed to be  $\text{S}_4$ ,  $\text{S}_5$ , and  $\text{S}_2$  (and not  $\text{S}_3$  or any singly-charged sulfur species), and of course  $\text{Na}^+$ . The electroactive species are primarily  $\text{S}_4$ ,  $\text{S}_5$ , and  $\text{S}_2$ . The overall discharge of a Na/S cell starts with essentially pure sulfur, but very soon a separate polysulfide phase forms, which is believed to be the seat of the electrochemical reactions, and a number of chemical equilibria. The sulfur-rich phase is believed to be involved via reaction with the polysulfide phase. The discharge reactions in the two-phase region ( $\text{Na}_2\text{S}_{5.2}$  and sulfur) are:

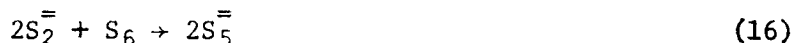
Electrochemical reduction of  $\text{Na}_2\text{S}_5$ ,<sup>20</sup> via a two-step reaction



Equilibria among the polysulfides and disproportionation of  $\text{S}_3^-$  (nonelectrochemical)



The sulfur phase reacts with the polysulfide phase, and is consumed in the process by such reactions as:



The potential of the sulfur electrode remains constant at about 2.075 V vs. sodium across this two-phase region of the phase diagram.

After all of the sulfur phase is consumed, the electrochemical reduction of polysulfides continues (with declining potential to about 1.75 V) through the single-phase region extending from  $\text{Na}_2\text{S}_{5.2}$  to  $\text{Na}_2\text{S}_3$  at about  $350^\circ\text{C}$ , according to Reactions 11 and 12 above, and the analogous two-step reduction of  $\text{S}_4^-$ :<sup>20</sup>





Reactions 11, 12, 18, and 19 are very fast, with exchange current densities in the  $1 \text{ A/cm}^2$  range. When the overall stoichiometry of the polysulfide melt reaches  $\text{Na}_2\text{S}_3$ ,  $\text{Na}_2\text{S}_2$  precipitates, blocking further access of melt to the electrolyte-current collector interface. Normally the discharge process is halted before this occurs.

The recharge process is believed to take place as follows, with the two-electron oxidation of  $\text{S}_4^{2-}$ :



followed by the reaction of sulfur with the polysulfide melt:



When the solubility limit for sulfur in polysulfide is exceeded, a separate sulfur phase is formed. At high current densities, this sulfur phase, being a poor electronic and ionic conductor, blocks further reaction as it is formed on the electrolyte and current collector. One problem in the design and operation of sulfur electrodes is to prevent this blockage by sulfur until the cell is nearly fully recharged. The voltage-capacity curves of Fig. 5 exhibit the behavior just discussed for the end of charge and end of discharge.<sup>21</sup>

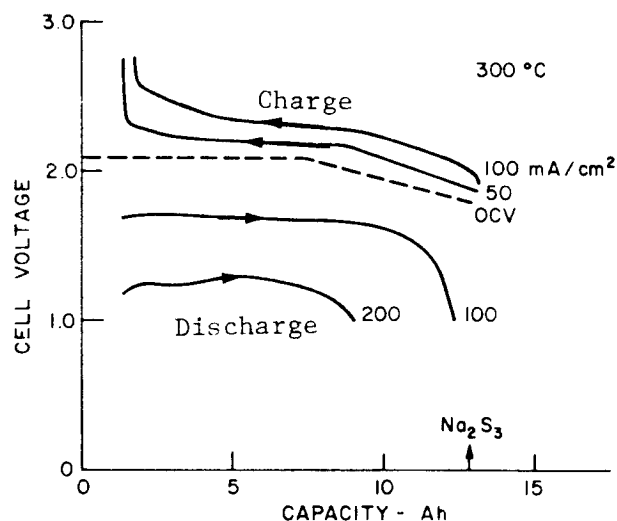


Fig. 5. Voltage-capacity curve for a Na/S cell at  $300^\circ\text{C}$ .<sup>21</sup>

The electrolytes which are used in sodium/sulfur cells are ceramics<sup>18-22</sup> or glasses<sup>23,24</sup> which conduct sodium ions. The glass electrolytes have rather low conductivity ( $\sim 5 \times 10^{-4} \Omega^{-1} \text{cm}^{-1}$ ), and must therefore be very thin ( $\sim 10 \mu\text{m}$ )

in order to yield a cell with an acceptably low internal resistance. In order to have an electrolyte geometry compatible with a  $10 \mu\text{m}$  thick electrolyte, hollow fibers ( $\sim 50 \mu\text{m}$ , OD) are used (Fig. 6). Thousands of borate glass fibers are bundled together with one end bonded to a low-melting  $\text{B}_2\text{O}_3\text{-Na}_2\text{O}$  glass "tube sheet," and the other end sealed. Sodium is fed to the insides of the hollow fibers from one side of the tube sheet. Among the fibers on their outsides are sulfur and a metal foil current collector.<sup>23</sup> The glass fibers are operated at a current density of  $2 \text{ mA/cm}^2$ , and have experienced failure by cracking after a number of charge-discharge cycles, and failure by cracking near the joint with the tube sheet. Thicker fiber walls favor longer cell lives. Recently,<sup>23</sup> glass fiber cells of the 1000-fiber,  $0.4 \text{ Ah}$  size have exhibited lifetimes of up to 3300 h, and cycle lives of 1600 cycles at 10-25% depth of discharge ( $\text{Na}_2\text{S}_3$  is 100%). Shorter lives are experienced at greater

depths of discharge.

The ceramic electrolytes for sodium/sulfur are composed of  $\text{Na}_2\text{O}$  and  $\text{Al}_2\text{O}_3$  in varying ratios in the range  $\text{Na}_2\text{O} \cdot 5\text{Al}_2\text{O}_3$  to  $\text{Na}_2\text{O} \cdot 11\text{Al}_2\text{O}_3$ , usually with small amounts of other oxides such as  $\text{Li}_2\text{O}$  or  $\text{MgO}$  to stabilize the  $\beta''$  structure<sup>19,21</sup> which is more conductive ( $3\text{--}5 \Omega \cdot \text{cm}$  at  $300^\circ\text{C}$ ) than the  $\beta$  structure<sup>22,25</sup> ( $20\text{--}30 \Omega \cdot \text{cm}$ ).

The  $\beta$ - and  $\beta''$ -alumina electrolytes (tubular, 1-3 cm OD, 1-2 mm wall, 10-30 cm long) can be prepared by a number of combinations of processing steps, as indicated by Table III. The overall process can be divided into three main steps: powder preparation, green body formation, and sintering. There are a number of options for each of the three main steps, however

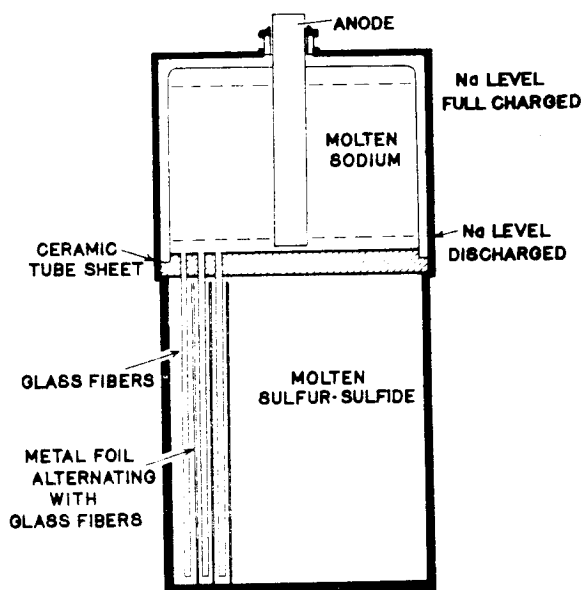


Fig. 6. Design of a hollow-glass-fiber Na/S cell.<sup>23</sup>

Table III.  $\beta$ - AND  $\beta''$ - $\text{Al}_2\text{O}_3$  FABRICATION METHODS

Powder Preparation	I	Direct mixing of compounds
	II	Decomposition of salt(s)
	III	Gel
	IV	Spray drying
	V	Complete reaction to $\beta$ - or $\beta''$ - $\text{Al}_2\text{O}_3$
Green Body Formation	A	Isostatic pressing
	B	Extrusion
	C	Electrophoretic deposition
Sintering Method	1	Encapsulated (in Pt or inert material)
	2	Enclosed with powder (high-temperature sintering)
	3	Zone pass-through

certain combinations of steps have been more popular than others:

IA1 has been used at Ford,<sup>21</sup> British Rail,<sup>19</sup> and others for preparation of  $\beta''$ - $\text{Al}_2\text{O}_3$

VC2 has been used by Compagnie Générale d'Electricite<sup>25</sup> and by General Electric<sup>26</sup> for  $\beta$ - $\text{Al}_2\text{O}_3$

IA3 has been used by Chloride Silent Power, and is being investigated in the Ford program<sup>21</sup> for  $\beta''$ - $\text{Al}_2\text{O}_3$ .

Powder preparation by methods II and III is being evaluated in the Ford program, as well as green body formation by method B, extrusion. Each major step

in electrolyte preparation has associated with it a number of important variables that have an influence on the chemical, microstructural and mechanical properties of the final product.

It is beyond the scope of this paper to review the details of  $\beta$ - $\text{Al}_2\text{O}_3$  electrolyte preparation, but some information on the major points is appropriate.

Powder Preparation: It is important to have fine-structured, uniformly mixed reactants. This is the objective of methods I-IV of Table III. The compositions favored<sup>21</sup> are in the range 9%  $\text{Na}_2\text{O}$ , 0.8%  $\text{Li}_2\text{O}$ , balance  $\text{Al}_2\text{O}_3$ , from  $\alpha$ - $\text{Al}_2\text{O}_3$ ,  $\text{Na}_2\text{CO}_3$  and  $\text{LiNO}_3$  starting materials.

Green Body Formation: The emphasis here is to prepare green bodies of optimum density with well-controlled tolerances and good uniformity for subsequent sintering to high density (>96% of theoretical).

Sintering: This may be the most difficult step in the process requiring minimum loss of  $\text{Na}_2\text{O}$  by volatilization at reaction-sintering temperatures in the range 1520-1600°C for a precise time (in the range 1 to 10 min), followed by annealing at a lower temperature ( $\sim 1400^\circ\text{C}$  for  $\sim 8$  h) to complete the formation of the  $\beta$ - $\text{Al}_2\text{O}_3$  phase with good conduction ( $\sim 5 \Omega\cdot\text{cm}$ ), but grain growth (beyond  $\sim 25 \mu\text{m}$ ) is to be avoided for good strength ( $\sim 1500 \text{ kg/cm}^2$ ).

Beta-alumina electrolytes have been operated in cells of various shapes and sizes, the most popular being tubular, with electrolytes about 1 cm diameter, and 1-2 mm thick. Various modes of failure of the electrolyte have been observed, the most common being sodium penetration from the sodium side toward the sulfur side, forming "fingers" of sodium which penetrate the electrolyte, eventually causing cracking. At the sulfur side, contamination of the beta alumina by potassium has been troublesome, causing cracking and flaking, as has been the formation of a thin coating of silica on the electrolyte, blocking the electrode reaction. Improvement of the purity and corrosion resistance of the sulfur electrode and housing extends the cell life considerably, as does improvement of the density and strength of the electrolyte.

Cells with two sodium electrodes have demonstrated lifetimes of more than 1000 A·h of charge passed per  $\text{cm}^2$  of electrolyte.<sup>21</sup> Carefully prepared Na/S laboratory cells (1-2 A·h size) containing no metals (avoiding iron, manganese, chromium, and silicon contamination) have sustained 600-1000 A·h of charge passed per  $\text{cm}^2$  corresponding to 4000-8000 cycles without any loss of capacity, as shown in Fig. 7.<sup>21</sup> However, these cells have been operating only in the single-phase ( $\text{Na}_2\text{S}_5$  to  $\text{Na}_2\text{S}_3$ ) region. This is impractical because it corresponds to a theoretical specific energy of only about 300 W·h/kg, which would probably result in a well-engineered cell of only 60-70 W·h/kg. Some cells with stainless steel containers have shown long lifetimes, but have suffered capacity loss because of silica coating of the electrolyte, and blockage of mass transport in the sulfur electrode because of the formation of solid lumps of iron, manganese, and chromium sulfides. Operation over the composition range S to  $\text{Na}_2\text{S}_3$  (or nearly so) corresponding to a more attractive theoretical specific energy of 756 W·h/kg has been difficult, especially during recharge, because of problems with segregation of polysulfide and formation of sulfur films on the electrolyte, resulting in capacity loss. Even with these problems, hundreds of cycles have been obtained (Table I), but with declining

capacity. Recent work with specially-shaped graphite current collectors for the sulfur electrode<sup>21</sup> has resulted in higher capacity densities at reasonably high current densities because of the promotion of favorable mass-transport conditions, avoiding the buildup of the products of electrochemical reaction at the electrolyte surface, and providing for the transport of reactant to the surface. Other interesting results include the use of metallic current collectors which are well wetted by polysulfide and not well wetted by sulfur, to promote more complete recharge.<sup>21</sup>

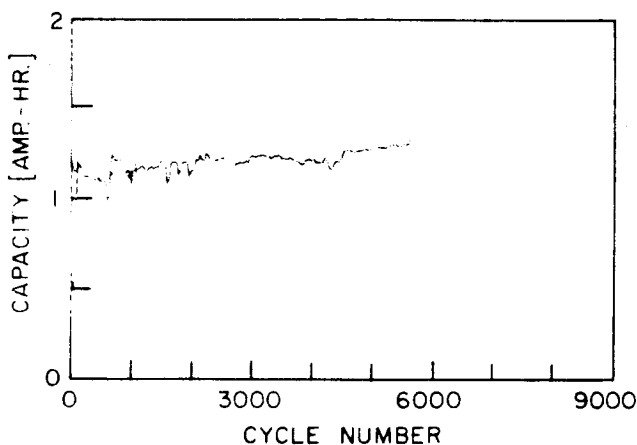


Fig. 7. Capacity-cycle number relationship for a long-lived, metal-free positive electrode Na/Na<sub>2</sub>S<sub>5.2</sub> cell.<sup>21</sup> Discharge current density 250 mA/cm<sup>2</sup>, charge current density 125 mA/cm<sup>2</sup>.

A few batteries of Na/S cells have been built and operated for relatively short periods of time, demonstrating in small sizes (15 A·h, 11 V, 165 W·h) a specific energy of 77 W·h/kg and a specific power of 154 W/kg exclusive of insulation, etc. A larger battery of 1000 cells<sup>27</sup> yielded 50 kW·h and a power of 20 kW, but with a high total system weight, so that the specific energy and specific power were not very high.<sup>28</sup>

The problems receiving emphasis for the Na/S cell are rather similar to those for the Li/MS cell. Corrosion-resistant metallic materials for use in contact with the sulfur electrode are needed for use as containers and possibly current collectors. A large number of materials have been tested, as shown in Table IV, with only graphite surviving well so far. A number of

Table IV. POSITIVE ELECTRODE MATERIALS FOR Na/S CELLS

Tested in Cells	Failure Mode	Reference
Material		
Stainless Steels	Mn Penetrates electrolyte Cr Blockage of ceramic and/or Fe current collector Si Oxide coats electrolyte	21
Carbon and Graphite	Stable - some interaction with corrosion products.	21
Aluminum (refractory metal coated)	Erratic results	29
Aluminum-Magnesium Alloy (carbon coated)	N.A. (2-year life)	23
Corrosion Resistant in Static Tests		
Cr <sub>2</sub> O <sub>3</sub> , oxide coated AISI 446 stainless steel, MoS <sub>2</sub> , ZrO <sub>2</sub> , La <sub>0.84</sub> Sr <sub>0.16</sub> CrO <sub>3</sub> , TiO <sub>2</sub> (single crystal) + Ta <sub>2</sub> O <sub>5</sub> , SrTiO <sub>3</sub> , CaTiO <sub>3</sub> + 3% Fe <sub>2</sub> O <sub>3</sub> , polyphenylene thermosetting resins.		21
Unstable		
TaB <sub>2</sub> , ZrC, VN, NbB <sub>2</sub> , ZrSi <sub>2</sub> , TiSi <sub>2</sub> , CrB <sub>2</sub> , ZrN, CrC, CaTiO <sub>3</sub> + 0.3% Fe <sub>2</sub> O <sub>3</sub> , TiC		21
ZrB <sub>2</sub> } with oxide film CrSi <sub>2</sub> }		
AISI 446 stainless steel		

other candidate materials have been identified in static corrosion tests, and await testing in cells. Chromium oxide is an interesting electronic conductor which might be useful as a coating on a stainless steel cell case. Other problems include the need for corrosion-resistant seals and feedthroughs, and improved joining techniques to seal beta alumina to alpha alumina. More work is needed on the operation of cells across the full composition range S to  $\text{Na}_2\text{S}_3$  at reasonable rates ( $>0.1 \text{ A/cm}^2$ ) without capacity loss for at least 1000 cycles. Of course, inexpensive fabrication procedures for the electrolyte are a necessity. As more work is carried out on battery design and operation, cell charge balancing techniques must be worked out, and thermal control methods must be perfected. These latter two areas are important for all high temperature cells.

#### SODIUM/METAL CHLORIDE CELLS

Another cell which has recently been investigated<sup>30,31</sup> that makes use of a beta alumina electrolyte is the  $\text{Na}/\beta\text{-Al}_2\text{O}_3/\text{M}_x\text{Cl}_y$  in  $\text{NaCl-AlCl}_3$  cell, which operates at temperatures near  $200^\circ\text{C}$ . During discharge, sodium is transferred to the  $\text{M}_x\text{Cl}_y$  compartment which contains  $\text{SbCl}_3$ ,  $\text{CuCl}_2$ ,  $\text{FeCl}_3$  or  $\text{NiCl}_3$  as the reactant. Cells have been assembled using either disk- or tube-shaped electrolyte. Early tests have been confined to relatively small ( $<10 \text{ A}\cdot\text{h}$ ) laboratory cells of low specific energy. Operating current densities of  $20 \text{ mA/cm}^2$  are typical.

Little information is available on cell performance, other than curves such as those of Fig. 8, which shows a voltage-capacity curve for operation at a constant current of 30 mA (the 18-h rate) for a  $0.56 \text{ A}\cdot\text{h}$  cell.<sup>30</sup> Disk electrolyte cells have achieved 5000 h and 200 cycles of operation whereas tubular electrolyte cells, failing by electrolyte penetration by sodium or by cracking have not yet demonstrated long life.<sup>31</sup> Information on voltage vs. current density has not been publicly available. At this workshop, additional information is expected to be provided.

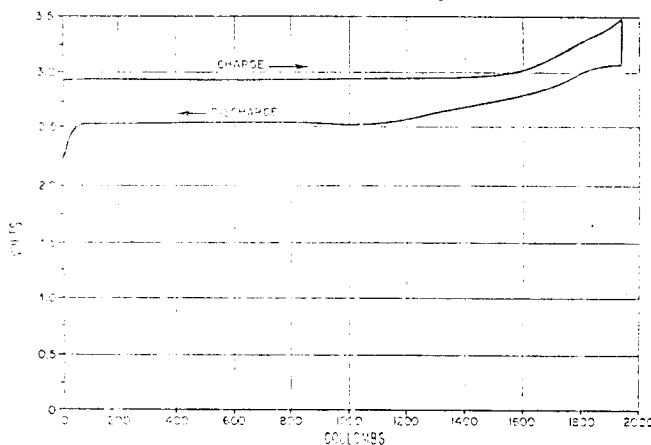


Fig. 8. Voltage-capacity curve for a  $\text{Na}/\beta\text{-Al}_2\text{O}_3/\text{M}_x\text{Cl}_y$  cell.<sup>30</sup>

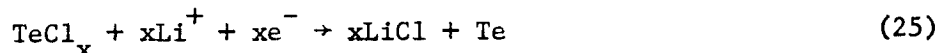
#### LITHIUM-ALUMINUM/C- $\text{TeCl}_4$ CELL

Investigation and development of the  $\text{Li-Al/LiCl-KCl/C-TeCl}_4$  cell operating at  $475^\circ\text{C}$  have been performed over about the last decade by Standard Oil (Ohio)<sup>32</sup> and more recently by ESB.<sup>33</sup> The negative electrode is 45 a/o Li-Al alloy, as discussed in the Lithium/Metal Sulfide Cells section of this paper. The electrolyte is the  $\text{LiCl-KCl}$  eutectic in a boron nitride cloth separator, and the positive electrode is a special porous carbon of high specific area, containing  $\text{TeCl}_4$ . The high-area carbon provides for the adsorption of chloride and alkali metal ions:





The  $\text{TeCl}_4$  adds to the capacity of the positive electrode by means of the following reactions:



The  $\text{TeCl}_4$  addition yields a flatter voltage plateau at about 2.7 V than is obtained from Reactions 23 and 24. Lightweight, sealed cells having two square, 58 cm negative electrodes between which is a two-sided positive electrode of equal area are now being constructed and tested. A typical voltage vs capacity curve is shown in Fig. 9.

Single cells have yielded specific energies as high as 79 W·h/kg. A 12-cell experimental battery weighing 5.4 kg delivered 264 W·h (49 W·h/kg) at the 2-h rate, and operated for 100 cycles over a period of about 300 h.<sup>32</sup> Currently, single cells are being constructed and tested after a pause in the program.

The problem areas for this cell are similar to those for other high-temperature cells: seals, feed-throughs, and materials, especially for the current collector of the positive electrode (where tungsten and graphite are now being used). An inherent difficulty for this system, because of the low capacity per unit weight of the positive electrode, is the low specific energy (45-60 W·h/kg); however, the high specific power capability is adequate (450 W/kg). It is expected that batteries of these cells will be constructed for testing in fork lift trucks in the future.<sup>33</sup>

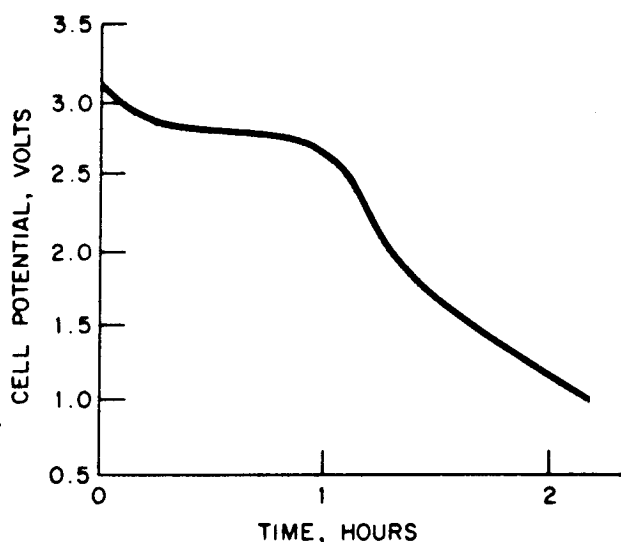


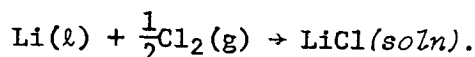
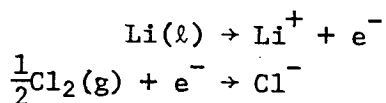
Fig. 9. Voltage-capacity curve for a Li-Al/C- $\text{TeCl}_4$  cell.<sup>32</sup> Discharge current: 6 A, area  $\sim 150 \text{ cm}^2$ .

#### LITHIUM/CHLORINE CELLS

Lithium/chlorine cells have been under investigation for over a decade, both as primary and as rechargeable cells. They make use of pure lithium held by capillary forces in a metallic current collector as the negative electrode, a molten  $\text{LiCl}$  or alkali halide mixture electrolyte, and a porous graphite chlorine electrode. Operating temperatures have been near  $650^\circ\text{C}$ , but have been reduced recently to  $450^\circ\text{C}$ .<sup>34</sup> The mixed alkali halide electrolyte which

has permitted the temperature reduction is 19 m/o LiF-66 m/o LiCl-15 m/o KCl.

The electrode reactions are very simple:



The cell potential is constant at about 3.6 V for the full capacity, in contrast to the situation for all other cells of this paper. The use of chlorine gas necessitates chlorine storage, which may be accomplished by adsorption on carbon.

A recent cell is shown in Fig. 10. Cells of this type have operated for periods up to 668 h, and 210 cycles at a capacity density of 0.34 A·h/cm<sup>2</sup>, corresponding to an impressive 277 W·h/kg, counting only the weight of the cell itself, without chlorine storage, insulation, etc.

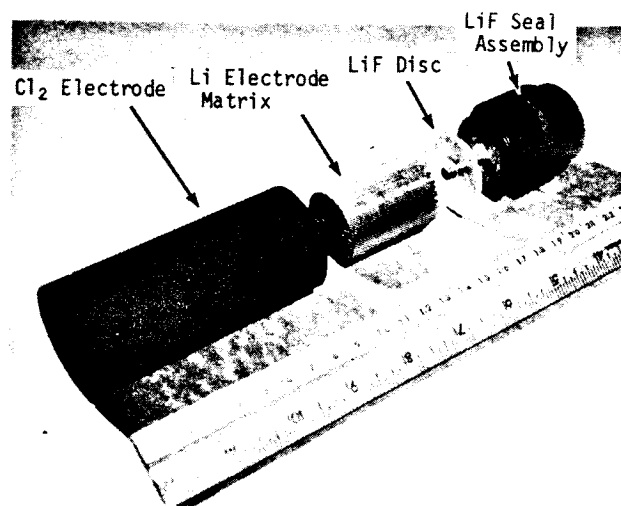


Fig. 10. Stackable Li/Cl<sub>2</sub> cell parts including a hot-pressed LiF seal.<sup>34</sup>

The problem areas for the lithium/chlorine cell are largely materials-related, because of the corrosive nature of the chlorine. Reliable seals and conductors are needed, as well as a simple, compact, lightweight means for chlorine storage and handling. The chlorine electrode gradually floods with electrolyte, a life-limiting factor. Control of this problem is essential.

#### SUMMARY AND PROJECTIONS

The status of high-temperature cell performance and lifetime is summarized in the right-hand portion of Table I. The systems which have shown the most rapid progress are those receiving the most effort: sodium/sulfur, and lithium alloy/metal sulfide. Both cells show promise of achieving 200 W·h/kg in the not-too-distant future. Some difficulty will probably be experienced in attempting to achieve that specific energy at a specific power approaching 200 W/kg. Single cells are now showing lifetimes of several thousand hours, and cycle lives of hundreds, over practical composition ranges. Figure 11 shows the specific power *vs.* specific energy curves for a number of electrochemical cells and heat engines. The difficulties with regard to the simultaneous achievement of high specific energy and high specific power for Li-Al/FeS and Na/S cells are reflected by the leftward curvature of the solid lines in Fig. 11. The progress in the last seven or eight years has been very good. The projected curves (dashed) represent expectations for the next several years. The prospects for continued progress look bright, but during this period, the difficult materials and seals problems must be solved, and the cost problems must be squarely faced.

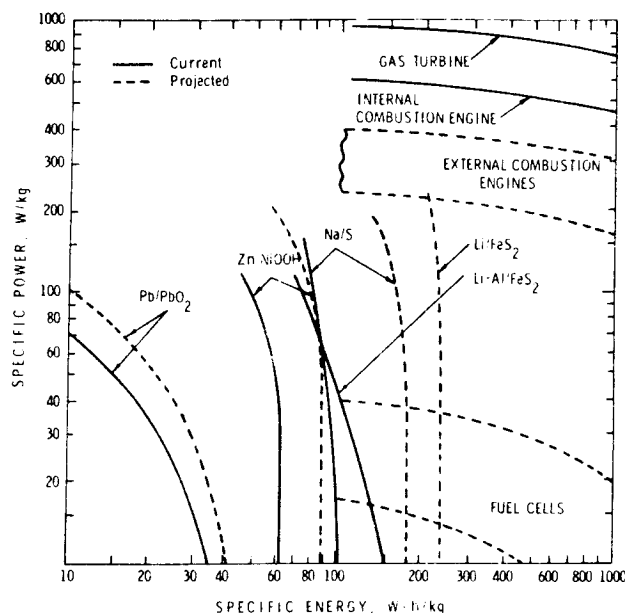


Fig. 11. Specific energy *vs.* specific power for various systems.

#### REFERENCES

1. E. J. Cairns and H. Shimotake, *Science*, **164**, 1347 (1969).
2. H. Shimotake and E. J. Cairns, Abstract 206, Electrochemical Society Extended Abstracts, Spring Meeting, New York, N. Y., May, 1969; also Extended Abstracts of the Battery Division, 5, 520 (1969).
3. E. J. Cairns, *et al.*, "Lithium/Sulfur Secondary Cells," presented at the 23rd Meeting of the Inter. Soc. of Electrochem., Stockholm, Sweden, Aug. 27-Sept. 2, 1972; also Extended Abstracts, ISE, p. 432 (1972).
4. D. R. Vissers, Z. Tomczuk, and R. K. Steunenbergh, *J. Electrochem. Soc.*, **121**, 665 (1974).
5. P. A. Nelson, E. C. Gay, and W. J. Walsh, in *Proc. 26th Power Sources Symposium*, PSC Publications Committee, Red Bank, N. J. (1974).
6. L. R. McCoy, *et al.*, in *Proc. 26th Power Sources Symposium*, PSC Publications Committee, Red Bank, N. J. (1974).
7. R. K. Steunenbergh, *et al.*, in P. A. Nelson, *et al.*, "High Performance Batteries for Off-Peak Energy Storage, ANL-8057, Argonne National Laboratory (November 1974), p. 21 ff.
8. R. K. Steunenbergh, *et al.*, in P. A. Nelson, *et al.*, "High Performance Batteries for Off-Peak Energy Storage, Jan.-June, 1974," ANL 8109, Argonne National Laboratory (January 1975), p. 77 ff.
9. P. A. Nelson, *et al.*, "High Performance Batteries for Off-Peak Energy Storage and Electric Vehicle Propulsion, July-Dec., 1974, ANL-75-1 (July 1975), p. 103 ff.
10. R. N. Seefurth and R. A. Sharma, *J. Electrochem. Soc.*, **122**, 1049 (1975).
11. W. J. Walsh, *et al.*, in *Proc. 9th IECEC*, Amer. Soc. of Mech. Eng'rs, New York, N. Y. (1974), p. 911.
12. E. C. Gay, F. J. Martino, and Z. Tomczuk, in *Proc. 10th IECEC*, Institute of Electrical and Electronics Engineers, New York, N. Y. (1975), p. 627.
13. S. Lai and L. R. McCoy, Abstract 21, Electrochemical Society Extended Abstracts, Fall Meeting, Dallas, Texas, October 1975.

14. S. D. James and L. E. DeVries, Abstract 22, Electrochemical Society Extended Abstracts, Fall Meeting, Dallas, Texas, October 1975.
15. C. C. McPheeters, W. W. Schertz, and N. P. Yao, Abstract 25, Electrochemical Society Extended Abstracts, Fall Meeting, Dallas, Texas, October 1975.
16. N. Koura, J. Kincinas, and N. P. Yao, Abstract 30, Electrochemical Society Extended Abstracts, Fall Meeting, Dallas, Texas, October 1975.
17. W. W. Schertz, *et al.*, in Proc. 10th IECEC, Institute of Electrical and Electronics Engineers, New York, N. Y. (1975), p. 634.
18. J. T. Kummer and N. Weber, Paper No. 670179, presented at the SAE Automotive Engineering Congress, Detroit, Mich., Jan. 9-13, 1967.
19. J. L. Sudworth, in Proc. 10th IECEC, Institute of Electrical and Electronics Engineers, New York, N. Y. (1975), p. 616.
20. R. P. Tischer and F. A. Ludwig, in "Advances in Electrochemistry and Electrochemical Engineering," V. 10, C. W. Tobias and H. Gerischer, editors, in press.
21. S. A. Weiner, *et al.*, "Research on Electrodes and Electrolyte for the Ford Sodium-Sulfur Battery," Ford Motor Co. Report to NSF, Annual Report for June, 1974 to June, 1975 (July, 1975).
22. J. Fally, *et al.*, J. Electrochem. Soc., 120, 1292 (1973).
23. C. A. Levine, in Proc. 10th IECEC, Institute of Electrical and Electronics Engineers, New York, N. Y. (1975), p. 621.
24. C. Levine, Proc. 25th Power Sources Symposium, PSC Publications Committee, Red Bank, N. J. (1972).
25. J. Fally, *et al.*, J. Electrochem. Soc., 120, 1296 (1973).
26. R. W. Powers, Report No. 73CRD289, General Electric Corp., Corporate R & D, October 1973.
27. R. W. Minck, Proc. 7th IECEC, Paper No. 729009, American Chemical Society, Washington, D.C. (September 1972).
28. "New Battery Will Double Range of Electrics," Commercial Motor, Nov. 10, 1972.
29. J. B. Bush, Jr., *et al.*, "Sodium-Sulfur Battery Development for Bulk Power Storage," Electric Power Research Institute, Research Report 128-2, September, 1975.
30. J. Werth, "Alkali Metal-Metal Chloride Battery," U.S. Patent 3,877,984, April 15, 1975.
31. J. J. Werth, "Sodium Chloride Battery Development Program for Load Leveling," Electric Power Research Institute, Research Report 109-2-1, June, 1975.
32. J. E. Metcalfe, E. J. Chaney, and R. A. Rightmire, in Proc. 1971 IECEC, Society of Automotive Engineers, New York, N. Y. (1971), p. 685.
33. J. C. Schaefer, *et al.*, in Proc. 10th IECEC, Institute of Electrical and Electronics Engineers, New York, N. Y. (1975), p. 649.
34. T. G. Bradley and R. A. Sharma, in Proc. 26th Annual Power Sources Symposium, PSC Publication Committee, Red Bank, N. J. (1974), p. 60.